Journal of Nuclear Materials 402 (2010) 25–29

Contents lists available at ScienceDirect

Journal of Nuclear Materials

journal homepage: www.elsevier.com/locate/jnucmat

Modeling the thermochemical behavior of AmO_{2-x}

Theodore M. Besmann *

Materials Science and Technology Division, Oak Ridge National Laboratory, 1 Bethel Valley Road, P.O. Box 2008, Oak Ridge, TN 37831-6063, USA

ARTICLE INFO

Article history:
Received 15 March 2010
Accepted 19 April 2010

ABSTRACT

A thermochemical representation of the fluorite structure AmO_{2-x} phase was developed using the compound energy formalism approach assuming constituents of $(Am^{4+})_1(O^{2-})_2$, $(Am^{4+})_1(Va)_2$, $(Am^{3+})_1(O^{2-})_2$, and $(Am^{3+})_1(Va)_2$. The Gibbs free energies for the constituents and a set of interaction parameters were determined using reported oxygen potential–temperature–composition data. A good fit to the experimental information was obtained which well-reproduces the behavior. The representation is also in a format that will allow incorporation of other dissolved metals and thus will be useful in generating multi-component compound energy formalism representations for complex oxide nuclear fuel and waste systems. A full assessment relating the fluorite structure phase to the phase equilibria for Am–O, however, must await adequate data for the remainder of the system.

1. Introduction

The objective of long-range nuclear energy programs around the world is to close the fuel cycle and recover the over 90% of the energy in fuel material that is currently disposed of in once-through fuel cycles. In addition to recovering usable fuel through recycle, the aim of many programs, including that in the US, is to consume transuranics to reduce proliferation concerns and reduce repository needs. Mixed oxide (MOX) fuel consisting of natural or depleted uranium with fissile plutonium, particularly for use in fast spectrum reactors, not only produces energy from an otherwise discarded actinide but also removes it as a potential source of clandestine weapons production. Including other transuranics in MOX fuel, or incorporating them into separate targets for irradiation in fast reactors, are also means of consuming the troublesome long-lived radionuclides so that wastes will be radiotoxic for orders of magnitude shorter period, for example the analysis of Westlen [1].

While there is substantial impetus to remove transuranics from spent fuel, include them in fuel forms or targets, and consume them in fast reactors there is limited understanding of the basic behavior of individual transuranics let alone multi-component systems. This is especially true of oxide fuels as these have the greatest international interest. The thermochemical properties and phase equilibria of these systems are particularly important as noted in recent reviews by Minato et al. [2] and Potter [3].

An effort to model the AmO_{2-x} phase was undertaken to provide basic information for use in the thermochemical and phase equilibrium modeling of transuranic fuel and targets. Experimental information is limited, with the high temperature information of interest largely oxygen pressure–temperature–composition. Using that information Thiriet and Konings [4] have modeled AmO_{2-x} with the associate species approach of Lindemer and Besmann, fitting the stoichiometry of a constituent species in a regular solution [5–8]. The objective of the effort reported here is to develop a model for the AmO_{2-x} phase using the compound energy formalism (CEF) [9] approach that addresses mixing of constituents on multiple sublattices and therefore may better represent the entropic behavior of the system, can be directly extended to multi-component systems, and is being used in the FUELBASE [10] international nuclear fuel modeling and database effort. Thus a CEF representation will also allow its integration with models for other actinides and fuel constituents to allow development of more complex, multi-component representations.

2. Am–O phase equilibria

A tentative phase diagram for the Am–O system is seen in Thiriet and Konings [4] which contains the oxide phase fcc AmO_{2-x}, the hexagonal and cubic phases for Am_2O_3, and the high temperature $AmO_{1.5+x}$ phase. Illustrated is the large homogeneity range for fcc AmO_{2-x} down to ~1300 K where a miscibility gap emerges. The phase also appears to extend from AmO_2 to $AmO_{1.6}$. An uncertain liquidus/solidus is shown above 2000 K.

Otobe et al. [11] reported extensive oxygen potential measurements at 1333 K across the composition range from $x = 0$ to 0.5 and measurements at several values of x over the 1000–1333 K range. They interpreted phase equilibria from values of x at 1333 K determining whether the oxygen potential remained constant or decreased with increasing x, with constant values indicating two-phase regions. They report two intermediate phases not indicated

* Tel.: +1 865 574 6852; fax: +1 865 574 4913.
E-mail address: besmanntm@ornl.gov

0022-3115/$ - see front matter © 2010 Elsevier B.V. All rights reserved.
doi:10.1016/j.jnucmat.2010.04.019

in earlier work nor in the phase diagram of Thiriet and Konings [4] of Am_7O_{12} and Am_9O_{16}. In the analogous ceria system the high temperature phase Ce_7O_{12} is present, yet homologous series phases such as the Ce_9O_{16} phase are stable only well below 1000 K based on determined phase equilibria and extensive assessments [12,13]. In addition, the oxygen potential plateau reported by Otobe which ostensibly indicates the two-phase regions AmO_{2-x}–Am_9O_{16} is very narrow and thus difficult to discern. It is also followed by a significant compositional region over which the oxygen potential continues to decrease implying a decreasing O/Am ratio and thus another highly defected phase between Am_7O_{12} and Am_9O_{16} for which there is no ceria analog [13].

3. CEF model for AmO_{2-x}

The actinide oxides in general have fluorite structure phases with significant homogeneity ranges. Americium like plutonium is found to only exhibit +3 and +4 valence as does analogous cerium, and thus they have a maximum oxygen–metal ratio of two. Zinkevich et al. [13] successfully used the CEF approach to represent the fluorite structure CeO_{2-x} and Gueneau et al. [14] similarly used a CEF model for PuO_{2-x}, in both cases developing a consistent computed phase diagram for the higher temperature regions of the Ce–O and Pu–O systems. Those approaches will similarly be used for the fluorite structure AmO_{2-x} phase.

Details of the CEF approach for AmO_{2-x} can be seen in Gueneau et al. [14] for PuO_{2-x} and much of the details will be left to that report. The technique utilizes a two sublattice approach such that

$$(Am^{3+}, Am^{4+})_1(O^{2-}, Va)_2$$

where the first sublattice has the cation lattice sites and the second is the anion and its site vacancies which are necessary to represent hypostoichiometry. The sublattice system is then considered as a solution of constituent species:

$(Am^{4+})_1(O^{2-})_2$
$(Am^{4+})_1(Va)_2$
$(Am^{3+})_1(O^{2-})_2$
$(Am^{3+})_1(Va)_2$.

Occupancy ratio is fixed as a single atom on the anion and two atoms (or vacancies) on the cation lattice with electroneutrality maintained through compensation of oxygen vacancies with Am^{3+} ions.

The approach is the same as that of Gueneau et al. [14] for PuO_{2-x} but differs somewhat from that of Zinkevich et al. [13] for CeO_{2-x} who treated the system as

$$(Ce^{3+}, Ce^{4+})_2(O^{2-}, Va)_4.$$

While the enthalpic terms for both stoichiometries are identical there is an entropic difference in mixing of the constituent species, with half as many mixing units for their CeO_{2-x} model than for the AmO_{2-x} model considered here.

The Gibbs free energy for AmO_{2-x} after Hillert [9] and as applied by Gueneau et al. [14] is

$$\begin{aligned} G = {} & y_{Am^{4+}}y_{O^{2-}}G_{Am^{4+}:O^{2-}} + y_{Am^{4+}}y_{Va}G_{Am^{4+}:Va} + y_{Am^{3+}}y_{O^{2-}}G_{Am^{3+}:O^{2-}} \\ & + y_{Am^{3+}}y_{Va}G_{Am^{3+}:Va} + RT(y_{Am^{3+}}\ln y_{Am^{3+}} + y_{Am^{4+}}\ln y_{Am^{4+}}) \\ & + 2RT(y_{O^{2-}}\ln y_{O^{2-}} + y_{Va}\ln y_{Va}) + G^{ex} \end{aligned} \quad (1)$$

where y_i is the site fraction for component i in the sublattice, G_i is the Gibbs free energy of the constituent species for the combinations of components on the sublattices, R is the ideal gas law constant, T is absolute temperature, and G^{ex} is the excess free energy due to interactions between the constituents. Using a first order Redlich–Kister–Muggianu expansion to represent the excess free energy it can be expressed as

$$\begin{aligned} G^{ex} = {} & y_{Am^{3+}}y_{Am^{4+}}L^0_{(Am^{3+},Am^{4+})_1(O^{2-})_2} + (y_{Am^{3+}} - y_{Am^{4+}})L^1_{(Am^{3+},Am^{4+})_1(O^{2-})_2} \\ & + L^0_{(Am^{3+},Am^{4+})_1(Va)_2} + (y_{Am^{3+}} - y_{Am^{4+}})L^1_{(Am^{3+},Am^{4+})_1(Va)_2} \end{aligned} \quad (2)$$

where L are the interaction energy parameters of the expansion.

The Gibbs free energies of two neutral end-members are defined from reported values for AmO_2, $AmO_{1.5}$, and O_2 such that

$$G_{AmO_2} = G_{(Am^{4+})_1(O^{2-})_2} \quad (3)$$

$$G_{AmO_{1.5}} = \frac{3}{4}G_{(Am^{3+})_1(O^{2-})_2} + \frac{1}{4}G_{(Am^{3+})_1(Va)_2} + 2RT\left(\frac{1}{4}\ln\frac{1}{4} + \frac{3}{4}\ln\frac{3}{4}\right) \quad (4)$$

While AmO_{2-x} has the fluorite (fcc) structure, $AmO_{1.5}$ is actually a type-C (bcc) phase and thus there is an inconsistency in mixing the two in this representation. The $AmO_{1.5}$ phase however, can be viewed as a defected fcc phase with oxygen vacancies causing the apparent bcc structure. Thus even though the phase structures are different, in the CEF approach these are mixed as a solution and energetic differences accommodated through optimization-determined adjustments to the Gibbs free energies. The initial Gibbs free energies for constituents consisting of cations and vacancies are, for simplicity, defined as the values for the oxide constituents less those for oxygen, thus

$$G_{(Am^{4+})_1(Va)_2} = G_{(Am^{4+})_1(O^{2-})_2} - G_{O_2} \quad (5)$$

$$G_{(Am^{3+})_1(Va)_2} = G_{(Am^{3+})_1(O^{2-})_2} - G_{O_2} \quad (6)$$

The Gibbs free energies for the four constituents of the CEF solution are defined

$$G_{(Am^{4+})_1(O^{2-})_2} = G_{AmO_2} \quad (7)$$

$$G_{(Am^{4+})_1(Va)_2} = G_{AmO_2} - G_{O_2} \quad (8)$$

$$G_{(Am^{3+})_1(Va)_2} = G_{AmO_{1.5}} - \frac{3}{4}G_{O_2} - 2RT\left(\frac{1}{4}\ln\frac{1}{4} + \frac{3}{4}\ln\frac{3}{4}\right) \quad (9)$$

$$G_{(Am^{3+})_1(O^{2-})_2} = G_{AmO_{1.5}} + \frac{1}{4}G_{O_2} - 2RT\left(\frac{1}{4}\ln\frac{1}{4} + \frac{3}{4}\ln\frac{3}{4}\right) \quad (10)$$

The values for G_{AmO_2} were taken from assessed and estimated values for enthalpy, entropy, and heat capacity of Thiriet and Konings [4] and $G_{AmO_{1.5}}$ values are from Cordfunke and Konings [15]. The G_{O_2} values are from the Scientific Group Thermodata Europe (SGTE) database [16]. Table 1 contains the free energies used in optimizing the model for AmO_{2-x}.

4. Oxygen potential measurement data

The most utilitarian data for thermochemical modeling of AmO_{2-x} are oxygen pressure or oxygen potential measurements as a function of temperature and composition. Oxygen potential is the chemical potential of oxygen in a system, defined as $\mu_{O_2} = RT\ln(p^*_{O_2})$ where $p^*_{O_2}$ is a dimensionless quantity defined by the oxygen pressure divided by the standard state pressure (1 bar). The largest and most consistent data set is that of Chikalla and Eyring [17] who determined dissociation pressures using thermogravimetric analysis (TGA) at a set of temperatures over the range 1139–1455 K and to O/Am values from 2 to approaching 1.8 Otobe et al. [11] have argued that the lower temperature measurements

Table 1
Input thermodynamic parameters and results of optimization.

G_{O_2} = −6960.6927	−51.183147T	−22.258620T ln T	−1.023867 × 10$^{-2}T^2$	1.339947 × 10$^{-6}T^3$	−76749.55T^{-1} (298.15 < T < 900 K)
−13136.0174	24.743297T	−33.557260T ln T	−1.234899 × 10$^{-3}T^2$	1.669433 × 10$^{-8}T^3$	539886T^{-1} (900 < T < 3700 K)
14154.6459	−51.485458T	−24.479780T ln T	−2.634759 × 10$^{-3}T^2$	6.015443 × 10$^{-8}T^3$	−15120935T^{-1} (3700 < T < 6000 K)
G_{AmO_2} = −954892.683	378.78423T	−66.8904T ln T	−9.55615E-03T^2	7.726E-07T^3	274415T^{-1} (298.15 < T < 6000 K)
$G_{AmO_{1.5}}$ = −867362.311	316.850412T	−56.965T ln T	−1.484250E-02T^2	575250T^{-1} (298.15 < T < 1000 K)	
−867320.894	441.493165T	−76.565T ln T	−8.932500E-04T^2	−1.976667E-07T^3	−2468500T^{-1} (1000 < T < 6000 K)
$G_{(Am^{4+})_1(O^{2-})_2} = G_{AmO_2} - 180464 + 84.3124T$					
$G_{(Am^{3+})_1(O^{2-})_2} + G_{(Am^{3+})_1(Va)_2} + G_{O_2} - 200193 + 96.3878T$					
$G_{(Am^{3+})_1(Va)_2} = G_{AmO_{1.5}} - 0.75GO_2 + 1.12467RT + 238330 - 19.261T$					
$G_{(Am^{4+})_1(Va)_2} = G_{AmO_2} - G_{O_2}$ - 316835					
$L^0_{(Am^{3+},Am^{4+})_1(O^{2-})_2} = L^0_{(Am^{3+},Am^{4+})_1(Va)_2} = -11811 + 60.743T$					
$L^1_{(Am^{3+},Am^{4+})_1(O^{2-})_2} = L^1_{(Am^{3+},Am^{4+})_1(Va)_2} = 114387 - 52.293T$					

of Chikalla and Eyring [17] are in error in not revealing the miscibility gap region for the AmO_{2-x} phase seen in the differential scanning calorimetric (DSC) measurements of Sari and Zamorani [18]. Otobe et al. [11] note that it may be due to the possibly long equilibration time necessary to obtain phase separation in that low temperature region and thus was missed in the TGA investigation. The oxygen potential values of Chikalla and Eyring [17] do smoothly decrease with decreasing O/Am even for measurements below the maximum miscibility gap temperature of ~1300 K reported by Sari and Zamorani [18]. At equilibrium in the two-phase region the oxygen potential values should remain constant across the composition range.

It is possible that the measurements of Sari and Zamorani [18] with regard to the maximum temperature of the miscibility gap region may be problematic, perhaps indicating too high a maximum gap temperature. For the analogous phases PrO_{2-x} [20] and CeO_{2-x} [12] the maximum miscibility gap temperatures are 888 K and 914 K, respectively. The maximum miscibility gap temperature for PuO_{2-x} has been reported as ~920 K by Sari et al. [19], ~930 K by Besmann and Lindemer [21], and 943 K in Wright's [22] critical assessment. Gueneau et al. [14] note Wright's [22] assessment, however their computed phase diagram has a maximum miscibility gap temperature of 1165 K. Thus the significantly higher miscibility gap maximum temperature of Sari and Zamorani [18] for AmO_{2-x} may be inconsistent with similar systems. As the experimental and assessed phase equilibria for analogous systems show maximum miscibility gap temperatures well below the lowest oxygen potential measurement temperatures of Chikalla and Eyring [17] it was presumed here that their data was taken in a single-phase region.

In their development of a representation for AmO_{2-x} Thiriet and Konings [4] solely used the data of Chikalla and Eyring [17]. They did review the measurements of Casalta et al. [23] concluding that the data was taken at relatively low temperatures and limited in number. Otobe et al. [11] also considered the data of Casalta et al. [23] which they found inconsistent with their own electromotive force (EMF) measurements. Otobe et al. [11] as well have made EMF measurements of oxygen potential as a function of composition in AmO_{2-x}, with their values predominantly determined at 1333 K.

5. Optimization of AmO_{2-x}

The data of Chikalla and Eyring were used with the Gibbs free energy functions of Table 1 to fit both corrections to the functions and zeroth and first order interaction parameters (L^0 and L^1). As assumed by Gueneau et al. [14] the values for L for (Am^{3+}, $Am^{4+})_1(O^{2-})_2$ were made equivalent to those for (Am^{3+}, $Am^{4+})_1(Va)_2$, for interactions among the cations on that lattice. The software package FactSage [24] was used for the optimization applying the Optisage module. Declared independent variables were temperature, total pressure, and composition with the dependent variable the log of the oxygen pressure as reported by Chikalla and Eyring [17]. Optimization calculations were performed with Am_2O_3 as a formation target.

6. Results

The use of the entire data set of 283 measurements of Chikalla and Eyring [17] made at seven discrete temperatures and the 26 data points of Otobe et al. [11] measured at 1333 K did not allow convergence to a solution. Examination of the values revealed that measurements very near stoichiometry were inconsistent, with multiple oxygen potential values at or very near an O/Am of 2. This is understandable given the extremely sensitive response of oxygen potential in the phase near stoichiometry. When a reduced data set was used which omitted 37 points from Chikalla and Eyring [17] that approached AmO_2 in composition the calculations converged to a reasonable solution. The data of Otobe et al. [11] were not used because of inconsistency between the data sets and the much more limited data of Otobe et al. [11]. The results of the optimization as adjustments to the Gibbs free energies of the constituents of the CEF model and the interaction energies are shown in Table 1.

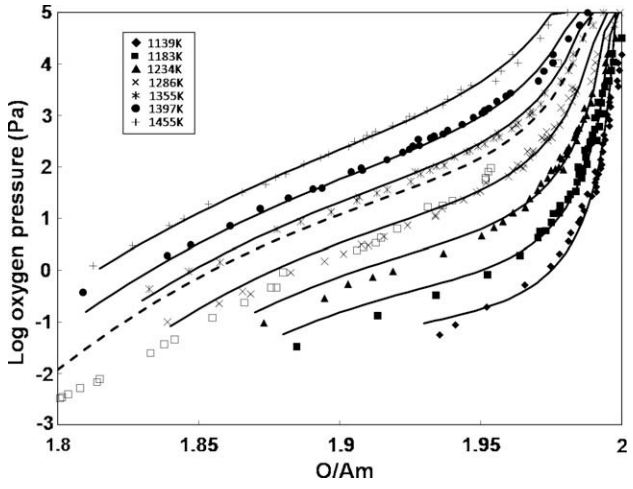

Fig. 1. Plot of experimental dissociation pressures of Chikalla and Eyring [17] (closed symbols) compared with results of the optimization of the CEF model for the AmO_{2-x} phase represented by the solid lines. The open symbols are the data of Otobe et al. [11] at 1333 K and the dashed line is the CEF model results at that temperature.

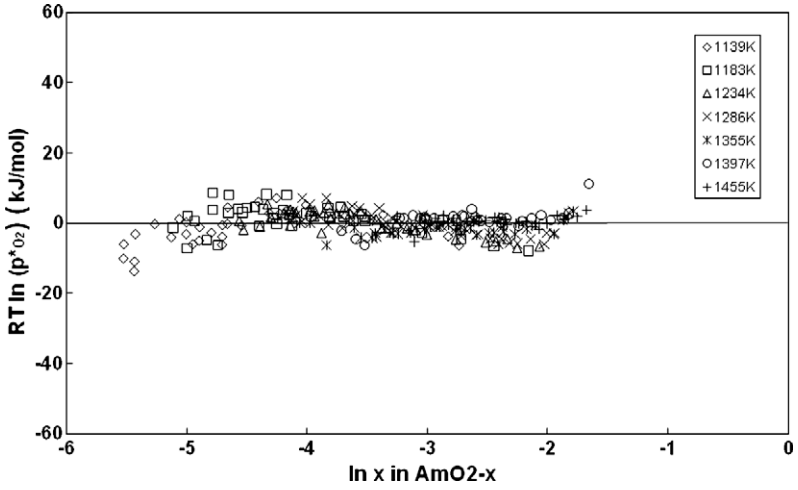

Fig. 2. Residuals for all the data of Chikalla and Eyring [17] relative to the CEF representation.

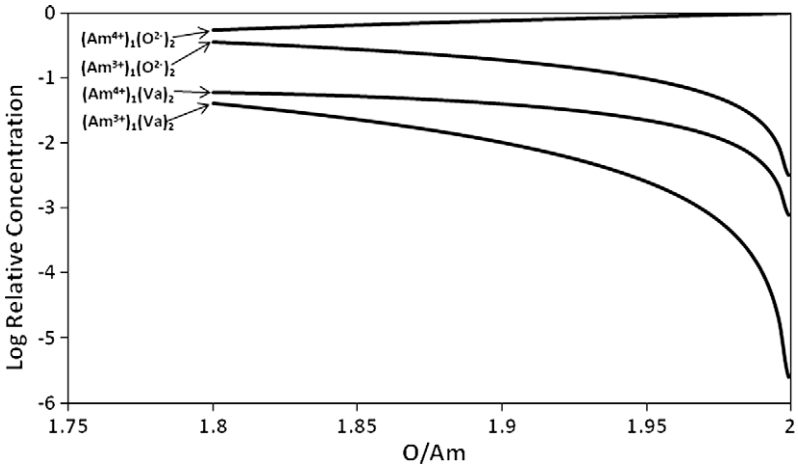

Fig. 3. The computed relative concentration of constituent CEF species in the representation as a function of composition.

A plot of the log of oxygen pressure versus O/Am in Fig. 1 shows all of Chikalla and Eyring's [17] 283 measurements and those of Otobe et al. [11] as well as computed pressures determined from the CEF model. Good agreement is seen between the Chikalla and Eyring [17] data and the calculated values. The results of Otobe et al. [11] however, are almost an order of magnitude lower in oxygen pressure than the model values. A plot of the residuals for all the Chikalla and Eyring data is seen in Fig. 2 and reflects good agreement with the derived model with a trend to larger residuals at small values of x. Optimization statistics indicate an agreement of chi square equal to 502.

The concentration of the model constituents as a function of composition are shown in Fig. 3. Little variation with temperature is seen over the range of the data utilized in the optimization, ~1000–1500 K. The dominant species is $(Am^{4+})_1(O^{2-})_2$ over O/Am = 1.8–2, with a significant concentration of $(Am^{3+})_1(O^{2-})_2$ at lower O/Am. The oxygen vacancy concentration is mostly provided by $(Am^{4+})_1(Va)_2$ with significant concentrations of $(Am^{3+})_1(Va)_2$ as well at lower O/Am.

7. Discussion

The fit to the data of Chikalla and Eyring in Fig. 1 is good, with especially good agreement for higher temperature measurements. The fit with the data at 1333 K of Otobe et al. [11] is not as reasonable, with the computed oxygen pressure almost an order of magnitude higher than the reported measurements. As noted above the discrepancy with Chikalla and Eyring's [17] results, may be due to the likelihood that their measurements are indeed in a single-phase region, however the lack of significant data at other temperatures precluded the use of Otobe et al. [11] data in the optimization.

The adjustments to the Gibbs free energies of the constituents that result from the optimization are fairly large and can be contrasted with those for CeO_{2-x} of Zinkevich et al. [13] and for PuO_{2-x} of Gueneau et al. [14]. In both cases they did not need to modify Gibbs free energies with the exception of $(Pu^{4+})_1(Va)_2$ which required a small adjustment. It is probable that the quality of the data for the component cerium and plutonium dioxide and sesquioxide phases is significantly better than for the americium phases given the substantially greater amount of measurements that have been performed on those systems. Naturally, the radioactivity and scarcity of americium is the cause of that discrepancy. Gueneau et al. [14] in similarly using the CEF approach for the $PuO_{1.61}$ phase which also has a considerable homogeneity range, did need to adjust the Gibbs free energies for all the constituents, including some very significantly. The values for the interaction parameters determined for AmO_{2-x} are also relatively large, but are of the same order as those for CeO_{2-x} [13] and PuO_{2-x} [14].

Thiriet and Konings [4] modeling AmO_{2-x} by an associates approach and the CEF technique using the data of Chikalla and Eyring [17] both resulted in reasonable representations. The plot of residuals in Fig. 2 can be compared with the similar plot in Fig. 7 of Thiriet and Konings [4] (plotted on the same scale to allow comparison). In both cases, again, the oxygen potentials at small values of x show the greatest discrepancy, and overall the CEF model appears to provide results with somewhat smaller residuals.

While the models of both Thiriet and Konings [4] and that presented here provide very useful representations for the phase, a full assessment of the Am–O system is still lacking. Given the paucity of thermochemical data on other Am–O phases and limited phase equilibria for the system such an assessment will need to await the reporting of significantly more experimental data or the development of first principles-derived information.

8. Conclusion

The CEF approach to modeling the thermochemical behavior of AmO_{2-x} was added to the already successful representation using associate species of Thiriet and Konings [4]. Experimental oxygen potential–temperature–composition data was used to optimize the CEF model, which well-reproduced the behavior. The CEF approach will also lend itself to allow incorporation of the AmO_{2-x} representation into multi-component representations of fluorite structure rare earth and actinide phases that will be important for modeling nuclear fuels and wastes. As Thiriet and Konings [4] note there is still uncertainty with regard to the miscibility gap for AmO_{2-x}. The limited thermochemical and phase equilibria data in the Am–O system and the disagreement among some measurements therefore does leave the system in some doubt. Given the importance of this and other transuranic systems for fuel recycle and waste disposal further work on these systems is warranted.

Acknowledgements

The authors are grateful to C. Thiriet for providing the tabulated data of Chikalla and Eyring and to Otobe for similarly providing their data in tabular form. Thanks also for the useful reviews by G.L. Bell, S.L. Voit, and P.C. Schuck. The research was supported by the US Department of Energy, Office of Nuclear Energy under the Fuel Cycle Research and Development and Nuclear Energy Advanced Modeling and Simulation programs.

This manuscript has been authored by UT-Battelle, LLC, under Contract No. DE-AC05-00OR22725 with the US Department of Energy. The United States Government retains and the publisher, by accepting the article for publication, acknowledges that the United States Government retains a non-exclusive, paid-up, irrevocable, world-wide license to publish or reproduce the published form of this manuscript, or allow others to do so, for United States Government purposes.

References

[1] D. Westlen, Prog. Nucl. Energy 49 (2007) 597–605.
[2] K. Minato, M. Takano, H. Otobe, T. Nishi, M. Akabori, Y. Arai, J. Nucl. Mater. 389 (2009) 23–28.
[3] P.J. Potter, Nucl. Mater. 389 (2009) 29–44.
[4] C. Thiriet, R.J.M. Konings, J. Nucl. Mater. 320 (2003) 292–298.
[5] T.M. Besmann, T.B. Lindemer, J. Nucl. Mater. 130 (1985) 489.
[6] T.B. Lindemer, T.M. Besmann, J. Nucl. Mater. 130 (1985) 473.
[7] T.B. Lindemer, J. Brynestad, J. Am. Ceram. Soc. 69 (1986).
[8] T.B. Lindemer, CALPHAD 10 (1986) 129.
[9] M. Hillert, J. Alloys Compd. 320 (2001) 161–176.
[10] C. Gueneau, D. Baichi, C. Labroche, B. Chatillon, B. Sundman, J. Nucl. Mater. 304 (2002) 161.
[11] H. Otobe, M. Akabori, K. Minato, J. Am. Ceram. Soc. 91 (2008) 1981–1985.
[12] M. Ricken, J. Nolting, J. Solid State Chem. 54 (1984) 89–99.
[13] M. Zinkevich, D. Djurovic, F. Aldinger, Solid State Ionics 177 (2006) 989–1001.
[14] C. Gueneau, C. Chatillon, B. Sundman, J. Nucl. Mater. 378 (2008) 257–272.
[15] E.H.P. Cordfunke, R.J.M. Konings, Reactor Materials and Fission Products, North Holland Elsevier Science Publishers B.B, The Netherlands, 1990. pp. 33–36.
[16] A.T. Dinsdale, CALPHAD 15 (4) (1991) 317.
[17] T.D. Chikalla, L. Eyring, J. Inorg. Nucl. Chem. 29 (1967) 2281.
[18] C. Sari, E. Zamorani, J. Nucl. Mater. 37 (1970) 324–330.
[19] C. Sari, U. Benedict, H. Blank, Thermodynamics of Nuclear Materials, IAEA, Vienna 1967,1968. pp. 587–611.
[20] L. Eyring, Sci. Technol. Rare Earth Mater. (1980) 99–118.
[21] T.M. Besmann, T.B. Lindemer, Trans. Am. Nucl. Soc. 50 (1985) 257.
[22] H.A. Wright, S. Bull, All. Ph. Dia. 11 (2) (1990) 184–202.
[23] S. Casalta, H. Matzke, C. Prunier, A thermodynamic properties study of the americium–oxygen system, in: Global 1995, ANS, vol. 2032, Paris, France, 1995, pp. 1667–1674.
[24] C.W. Bale, P. Chartrand, S.A. Degterov, S. Eriksson, K. Hack, R.B. Mahfoud, J. Melancon, A.D. Pelton, S. Petersen, CALPHAD 26 (2002) 39.